

## **A comparison of performance of several artificial intelligence methods for forecasting monthly discharge time series**

### **Wen-Chuan Wang**

Ph.D., Institute of hydropower system & Hydroinformatics, Dalian University of Technology, Dalian, 116024, P.R. China

Faculty of Water conservancy Engineering, North China Institute of Water Conservancy and Hydroelectric Power, Zhengzhou 450011, P.R.China

### **Kwok-Wing Chau**

Associate Professor, Department of Civil and Structural Engineering, Hong Kong Polytechnic University, Hung Hom, Kowloon, Hong Kong (Corresponding author): E-mail address: [cekwchau@polyu.edu.hk](mailto:cekwchau@polyu.edu.hk) Tel.: (+852) 2766 6014

### **Chun-Tian Cheng**

Professor, Institute of hydropower system & Hydroinformatics, Dalian University of Technology, Dalian, 116024, P.R. China

### **Lin Qiu**

Professor, Institute of environmental & municipal engineering, North China Institute of Water Conservancy and Hydroelectric power, ZhengZhou, 450011, P.R.Ch

**Abstract.** Developing a hydrological forecasting model based on past records is crucial to effective hydropower reservoir management and scheduling. Traditionally, time series analysis and modeling is used for building mathematical models to generate hydrologic records in hydrology and water resources. Artificial intelligence (AI), as a branch of computer science, is capable of analyzing long-series and large-scale hydrological data. In recent years, it is one of front issues to apply AI technology to the hydrological forecasting modeling. In this paper, autoregressive moving-average (ARMA) models, artificial neural networks (ANNs) approaches, adaptive neural-based fuzzy inference system (ANFIS) techniques, genetic programming (GP) models and support vector machine (SVM) method are examined using the long-term observations of monthly river flow discharges. The four quantitative standard statistical performance evaluation measures, the coefficient of correlation (R), Nash-Sutcliffe efficiency coefficient (E), root mean squared error (RMSE), mean absolute percentage error (MAPE), are employed to evaluate the performances of various models developed. Two case study river sites are also provided to illustrate their respective performances. The results indicate that the best performance can be obtained by ANFIS, GP and SVM, in terms of different evaluation criteria during the training and validation phases.

**Key words:** monthly discharge time series forecasting; ARMA; ANN; ANFIS; GP; SVM

## 42 **1. Introduction**

43 The identification of suitable models for forecasting future monthly inflows to hydropower  
44 reservoirs is a significant precondition for effective reservoir management and scheduling. The  
45 results, especially in long-term prediction, are useful in many water resources applications such as  
46 environment protection, drought management, operation of water supply utilities, optimal  
47 reservoir operation involving multiple objectives of irrigation, hydropower generation, and  
48 sustainable development of water resources, etc. As such, hydrologic time series forecasting has  
49 always been of particular interest in operational hydrology. It has received tremendous attention of  
50 researchers in last few decades and many models for hydrologic time series forecasting have been  
51 proposed to improve the hydrology forecasting.

52 These models can be broadly divided into three groups: regression based methods, time series  
53 models and AI-based methods. For autoregressive moving-average models (ARMA) proposed by  
54 Box and Jenkins (1970), it is assumed that the times series is stationary and follows the normal  
55 distribution. ARMA is one of the most popular hydrologic times series models for reservoir design  
56 and optimization. Extensive application and reviews of the several classes of such models  
57 proposed for the modelling of water resources time series were reported (Chen and Rao, 2002;  
58 Salas, 1993; Srikanthan and McMahon, 2001).

59 In recent years, AI technique, being capable of analysing long-series and large-scale data,  
60 has become increasingly popular in hydrology and water resources among researchers and  
61 practicing engineers. Since the 1990s, artificial neural networks (ANNs), based on the  
62 understanding of the brain and nervous systems, was gradually used in hydrological prediction. An  
63 extensive review of their use in the hydrological field is given by ASCE Task Committee on  
64 Application of Artificial Neural Networks in Hydrology (ASCE, 2000a; ASCE, 2000b). The ANNs  
65 have been shown to give useful results in many fields of hydrology and water resources research  
66 (Campolo et al., 2003; Chau, 2006; Muttil and Chau, 2006).

67 The adaptive neural-based fuzzy inference system (ANFIS) model and its principles, first  
68 developed by Jang (1993), have been applied to study many problems and also in hydrology field  
69 as well. Chang & Chang (2001) studied the integration of a neural network and fuzzy arithmetic  
70 for real-time streamflow forecasting and reported that ANFIS helps to ensure more efficient  
71 reservoir operation than the classical models based on rule curve. Bazartseren et al. (2003) used  
72 neuro-fuzzy and neural network models for short-term water level prediction. Dixon (2005)  
73 examined the sensitivity of neuron-fuzzy models used to predict groundwater vulnerability in a  
74 spatial context by integrating GIS and neuro-fuzzy techniques. Other researchers reported good  
75 results in applying ANFIS in hydrological prediction (Cheng et al., 2005; Keskin et al., 2006;  
76 Nayak et al., 2004).

77 Genetic Programming (GP), an extension of the well known field of genetic algorithms (GA)  
78 belonging to the family of evolutionary computation, is an automatic programming technique for  
79 evolving computer programs to solve problems (Koza, 1992). GP model was used to emulate the  
80 rainfall-runoff process (Whigam and Crapper, 2001) and was evaluated in terms of root mean  
81 square error and correlation coefficient (Liong et al., 2002; Whigam and Crapper, 2001). It was  
82 shown to be a viable alternative to traditional rainfall runoff models. The GP approach was also  
83 employed by Johari et al (2006) to predict the soil-water characteristic curve of soils. GP is  
84 employed for modelling and prediction of algal blooms in Tolo Harbour, Hong Kong (Muttil and

85 Chau, 2006) and the results indicated good predictions of long-term trends in algal biomass. The  
86 Darwinian theory-based GP approach was suggested for improving fortnightly flow forecast for a  
87 short time-series (Sivapragasam et al., 2007).

88 The support vector machine (SVM) is based on structural risk minimization (SRM) principle  
89 and is an approximation implementation of the method of SRM with a good generalisation  
90 capability (Vapnik, 1998). Although SVM has been used in applications for a relatively short time,  
91 this learning machine has been proven to be a robust and competent algorithm for both  
92 classification and regression in many disciplines. Recently, the use of the SVM in water resources  
93 engineering has attracted much attention. Dibike et al. (2001) demonstrated its use in rainfall  
94 runoff modeling. Liong and Sivapragasam (2002) applied SVM to flood stage forecasting in  
95 Dhaka, Bangladesh and concluded that the accuracy of SVM exceeded that of ANN in  
96 one-lead-day to seven-lead-day forecasting. Yu et al.(2006) successfully explored the usefulness of  
97 SVM based modelling technique for predicting of real time flood stage forecasting on Lan-Yang  
98 river in Taiwan 1 to 6 hours ahead. Khan and Coulibaly (2006) demonstrated the application of  
99 SVM to time series modeling in water resources engineering for lake water level prediction. The  
100 SVM method has also been employed for stream flow predictions (Asefa et al., 2006; Lin et al.,  
101 2006).

102 The major objectives of the study presented in this paper are to investigate several AI  
103 techniques for modelling monthly discharge time series, which include ANN approaches, ANFIS  
104 techniques, GP models and SVM method, and to compare their performance with other traditional  
105 time series modelling techniques such as ARMA. Four quantitative standard statistical  
106 performance evaluation measures, i.e., coefficient of correlation (R), Nash-Sutcliffe efficiency  
107 coefficient (E), root mean squared error (RMSE), mean absolute percentage error (MAPE), are  
108 employed to validate all models. Brief introduction and model development of these AI methods  
109 are also described before discussing the results and making concluding remarks. The performances  
110 of various models developed are demonstrated by forecasting monthly river flow discharges in  
111 Manwan Hydropower and Hongjiadu Hydropower.

## 112 **2 Description of Selected Models**

113 Several AI techniques employed in this study include ANNs, ANFIS techniques, GP models and  
114 SVM method. A brief overview of these techniques is presented here.

### 115 **2.1 Artificial Neural Networks (ANNs)**

116 Since early 1990s, ANNs, and in particular, feed-forward back-propagation perceptrons have been  
117 used for forecasting in many areas of science and engineering (Chau and Cheng, 2002). An ANN  
118 is an information processing system composed of many nonlinear and densely interconnected  
119 processing elements or neurons, which is organized as layers connected via weights between  
120 layers. An ANN usually consists of three layers: the input layer, where the data are introduced to  
121 the network; the hidden layer or layers, where data are processed; and the output layer, where the  
122 results of given input are produced. The structure of a feed-forward ANN is shown in Fig. 1.

123 A multi-layer feed-forward back-propagation network with one hidden layer has been used

124 throughout the study (Haykin, 1999). In a feed-forward back-propagation network, the weighted  
125 connections feed activations only in the forward direction from an input layer to the output layer.  
126 These interconnections are adjusted using an error convergence technique so that the network's  
127 response best matches the desired response. The main advantage of the ANN technique over  
128 traditional methods is that it does not require information about the complex nature of the  
129 underlying process under consideration to be explicitly described in mathematical form.

## 130 **2.2 Adaptive neural-based fuzzy inference system (ANFIS)**

131 The ANFIS used in the study is a fuzzy inference model of Sugeno type, and is a  
132 composition of ANNs and fuzzy logic approaches (Jang, 1993; Jang et al., 1997). The model  
133 identifies a set of parameters through a hybrid learning rule combining the back-propagation  
134 gradient descent and a least squares method. It can be used as a basis for constructing a set of  
135 fuzzy IF-THEN rules with appropriate membership functions in order to generate the previously  
136 stipulated input-output pairs (Keskin et al., 2006).

137 The Sugeno fuzzy inference system is computationally efficient and works well with linear  
138 techniques, optimization and adaptive techniques. As a simple example, we assume a fuzzy  
139 inference system with two inputs  $x$  and  $y$  and one output  $z$ . The first-order Sugeno fuzzy model, a  
140 typical rule set with two fuzzy If-Then rules can be expressed as:

141 Rule 1: If  $x$  is  $A_1$  and  $y$  is  $B_1$ , then  $f_1 = p_1x + q_1y + r_1$

142 Rule 2: If  $x$  is  $A_2$  and  $y$  is  $B_2$ , then  $f_2 = p_2x + q_2y + r_2$

143 The resulting Sugeno fuzzy reasoning system is shown in Fig. 2. It illustrates the fuzzy  
144 reasoning mechanism for this Sugeno model to derive an output function ( $f$ ) from a given input  
145 vector  $[x, y]$ . The corresponding equivalent ANFIS architecture is a five-layer feed forward net  
146 work that uses neural net work learning algorithms coupled with fuzzy reasoning to map an input  
147 space to an output space. It is shown in Fig.3. The more comprehensive presentation of ANFIS for  
148 forecasting hydrological time series can be found in the literature (Cheng et al., 2005; Keskin et al.,  
149 2006; Nayak et al., 2004).

## 150 **2.3 Genetic programming (GP)**

151 GP is a search methodology belonging to the class of 'intelligent' methods which allows the  
152 solution of problems by automatically generating algorithms and expressions. These expressions  
153 are codified or represented as a tree structure with its terminals (leaves) and nodes (functions). GP,  
154 similar to GA, initializes a population that compounds the random members known as  
155 chromosomes (individual). Afterward, fitness of each chromosome is evaluated with respect to a  
156 target value. GP works with a number of solution sets, known collectively as a "population",  
157 rather than a single solution at any one time; the possibility of getting trapped in a "local  
158 optimum" is thus avoided. GP differs from the traditional GA in that it typically operates on parse  
159 trees instead of bit strings. A parse tree is built up from a terminal set (the variables in the problem)  
160 and a function set (the basic operators used to form the function). GP is provided with evaluation  
161 data, a set of primitives and fitness functions. The evaluation data describe the specific problem in

162 terms of the desired inputs and outputs. They are used to generate the best computer program to  
 163 describe the relationship between the input and output very well (Koza, 1992).

164 The representation of GP can be viewed as a parse tree-based structure composed of the  
 165 function set and terminal set. The function set is the operators, functions or statements such as  
 166 arithmetic operators ( $\{+, -, *, /\}$ ) or conditional statements (if... then...) which are available in the  
 167 GP. The terminal set contains all inputs, constants and other zero-argument in the GP tree. An  
 168 example of such a parse tree can be found in Fig. 4. Once a population of the GP tree is initialized,  
 169 the following procedures are similar to GAs including defining the fitness function, genetic  
 170 operators such as crossover, mutation and reproduction and the termination criterion, etc. In GP,  
 171 the crossover operator is used to swap the subtree from the parents to reproduce the children using  
 172 mating selection policy rather than exchanging bit strings as in GAs.

173 The genetic programming introduced here is one of the simplest forms available. A more  
 174 comprehensive presentation of GP can be found in the literature (Borrelli et al., 2006; Koza,  
 175 1992).

## 176 2.4 Support vector machine (SVM)

177 SVM is the state-of-the-art neural network technology based on statistical learning (Vapnik, 1995;  
 178 Vapnik, 1998). The basic idea of SVM is to use linear model to implement nonlinear class  
 179 boundaries through some nonlinear mapping of the input vector into the high-dimensional feature  
 180 space. The linear model constructed in the new space can represent a nonlinear decision boundary  
 181 in the original space. In the new space, SVM constructs an optimal separating hyperplane. If the  
 182 data is linearly separated, linear machines are trained for an optimal hyperplane that separates the  
 183 data without error and into the maximum distance between the hyperplane and the closest training  
 184 points. The training points that are closest to the optimal separating hyperplane are called support  
 185 vectors. Fig. 5 exhibits the basic concept of SVM. There exist uncountable decision functions, i.e.  
 186 hyperplanes, which can effectively separate the negative and positive data set (denoted by 'x' and  
 187 'o', respectively) that has the maximal margin. This indicates that the distance from the closest  
 188 positive samples to a hyperplane and the distance from the closest negative samples to it will be  
 189 maximized.

190 Given a set of training data  $\{(x_i, d_i)\}_i^N$  ( $x_i$  is the input vector,  $d_i$  is the desired value and  $N$  is the  
 191 total number of data patterns), the regression function of SVM is formulated as follows:

$$192 \quad y = f(x) = w_i \phi_i(x) + b \quad (1)$$

193 where  $\phi_i(x)$  is the feature of inputs, and  $w_i$  and  $b$  are coefficients. The coefficients  
 194 ( $w_i$  and  $b$ ) are estimated by minimizing the following regularized risk function (Vapnik,  
 195 1995; Vapnik, 1998):

$$196 \quad r(C) = C \frac{1}{N} \sum_{i=1}^N L_\varepsilon(d_i, y_i) + \frac{1}{2} \|\omega\|^2 \quad (2)$$

197 where

$$198 \quad L_\varepsilon(d, y) = \begin{cases} |d - y| - \varepsilon & \text{if } |d - y| \geq \varepsilon \\ 0 & \text{otherwise} \end{cases} \quad (3)$$

199 In Eq. (2), the first term is the empirical error (risk). They are measured by Eq. (3).  $L_\varepsilon(d, y)$  is  
 200 called the  $\varepsilon$ -insensitive loss function, the loss equals zero if the forecast value is within the  
 201  $\varepsilon$ -tube and Fig. 6. The second term is used as a measure of the flatness of the function,  
 202 Hence, C is referred to as the regularized constant and it determines the trade-off between  
 203 the empirical risk and the regularization term. Increasing the value of C will result in an  
 204 increasing relative importance of the empirical risk with respect to the regularization term.  
 205  $\varepsilon$  is called the tube size and it is equivalent to the approximation accuracy placed on the  
 206 training data points. Both C and  $\varepsilon$  are user-prescribed parameters, two positive slack  
 207 variables  $\xi$  and  $\xi^*$ , which represent the distance from actual values to the corresponding  
 208 boundary values of  $\varepsilon$ -tube (Fig. 6), are introduced. Then, Eq. (2) is transformed into the  
 209 following constrained form.

$$210 \quad \text{Minimize: } \frac{1}{2} \|\omega\|^2 + C \left( \sum_i^N (\xi_i + \xi_i^*) \right) \quad (4)$$

$$211 \quad \text{Subject to } \begin{cases} \omega_i \phi(x_i) + b_i - d_i \leq \varepsilon + \xi_i^*, i = 1, 2, \dots, N \\ d_i - \omega_i \phi(x_i) - b_i \leq \varepsilon + \xi_i, i = 1, 2, \dots, N \\ \xi_i, \xi_i^*, i = 1, 2, 3, \dots, N \end{cases}$$

212 This constrained optimization problem is solved using the following primal Lagrangian form:

$$213 \quad L = \frac{1}{2} \|\omega\|^2 + C \left( \sum_i^N (\xi_i + \xi_i^*) \right) - \sum_i^N \alpha_i [\omega_i \phi(x_i) + b - d_i + \varepsilon + \xi_i] \\ 214 \quad - \sum_{i=1}^N \alpha_i^* [d_i - \omega_i \phi(x_i) - b + \varepsilon + \xi_i^*] - \sum_i^N (\beta_i \xi_i + \beta_i^* \xi_i^*) \quad (5)$$

215 Eq. (5) is minimized with respect to primal variables  $\omega_i, b, \xi$  and  $\xi^*$ , and maximized with  
 216 respect to the nonnegative Lagrangian multipliers  $\alpha_i, \alpha_i^*, \beta_i$  and  $\beta_i^*$ , Finally, Karush-Kuhn-  
 217 Tucker conditions are applied to the regression, and Eq. (5) has a dual Lagrangian form:

$$218 \quad \nu(\alpha_i, \alpha_i^*) = \sum_{i=1}^N d_i (\alpha_i - \alpha_i^*) - \varepsilon \sum_{i=1}^N (\alpha_i + \alpha_i^*) - \frac{1}{2} \sum_{i=1}^N \sum_{j=1}^N (\alpha_i - \alpha_i^*) (\alpha_j - \alpha_j^*) K(x_i, x_j) \quad (6)$$

219 with the constraints,

$$220 \quad \sum_{i=1}^N (\alpha_i - \alpha_i^*) = 0 \quad \text{And } \alpha_i, \alpha_i^* \in [0, C], i = 1, 2, \dots, N$$

221 In Eq. (6), the Lagrange multipliers satisfy the equality  $\alpha_i \alpha_i^* = 0$ , The Lagrange multipliers  
 222  $\alpha_i$  and  $\alpha_i^*$  are calculated, and the optimal desired weight vector of the regression hyperplane is

$$223 \quad \omega^* = \sum_{i=1}^N (\alpha_i - \alpha_i^*) K(x, x_i) \quad (7)$$

224 Therefore, the regression function can be given as

$$225 \quad f(x, \alpha, \alpha^*) = \sum_{i=1}^N (\alpha_i - \alpha_i^*) K(x, x_i) + b \quad (8)$$

226 Here,  $K(x, x_i)$  is called the Kernel function. The value of the Kernel is inner product of the two  
227 vectors  $x_i$  and  $x_j$  in the feature space  $\phi(x)$  and  $\phi(x_j)$ , so  $K(x, x_j) = \phi(x) \cdot \phi(x_j)$ , and function  
228 that satisfies Mercer's condition (Vapnik, 1998) can be used as the Kernel Function. In general,  
229 three kinds of kernel function are used as follows:

230 Polynomial:

$$231 \quad K(x, x_j) = (x \cdot x_j + 1)^n \quad (9)$$

232 Radial basis function (RBF)

$$233 \quad K(x, x_j) = \exp(-\|x - x_j\|^2 / 2\sigma^2) \quad (10)$$

234 Two-layer neural networks

$$235 \quad K(x, x_j) = \tanh(kx \cdot x_j - \delta)^n \quad (11)$$

### 236 **3 Study area and data**

237 In this study, Manwan Hydropower in Lancangjiang River is selected as a study site. The  
238 monthly flow data from January 1953 to December 2004 are studied. The data set from January  
239 1953 to December 1999 is used for calibration whilst that from January 2000 to December 2004 is  
240 used for validation (Fig.7). Lancangjiang River is a large river in Asia, which originates from  
241 Qinghai-Tibet Plateau, penetrates Yunnan from northwest to the south and passes through Laos,  
242 Burma, Thailand, Cambodia and Vietnam, ingresses into South China Sea finally. The river is  
243 about 4,500 km long and has a drainage area of 744,000 km<sup>2</sup>. Manwan Hydropower merges on the  
244 middle reaches of Lancang River and at borders of Yunxian and Jingdong counties. The catchment  
245 area at Manwan dam site is 114,500 km<sup>2</sup>, the length above Manwan is 1,579 km, and the mean  
246 elevation is 4,000 km. The average yearly runoff is 1,230 cubic meters per at the dam site. Rainfall  
247 provides most of the runoff and snow melt accounts for 10%. Nearly 70% of the annual rainfall  
248 occurs from June to September. Locations of Lancang River and Manwan Hydropower are shown  
249 in Fig.8 (A).

250 The second study site is at Hongjiadu Hydropower on Wujiang River in southwest China. The  
251 monthly flow data from January 1951 to December 2004 are studied. The data set from January  
252 1951 to December 1994 is used for calibration whilst that from January 1995 to December 2004 is  
253 used for validation (Fig.9). Wujiang River, originating from Wumeng foothill of Yun-Gui Plateau,  
254 is the biggest branch at the southern bank of Yangtze River, which covers 87,920km<sup>2</sup>, total length  
255 of 1,037km, centralized fall of 2,124m, and with approved installed capacity 8,800MW. Nowadays,  
256 Hongjiadu hydropower station is the master regulation reservoir for the cascade hydropower  
257 stations on Wujiang River. The catchment area at Hongjiadu dam site is 9,900 km<sup>2</sup> and the average  
258 yearly runoff is 155 cubic meters at the dam site. Rainfall provides most of the runoff. Locations  
259 of Wujiang River and Hongjiadu Hydropower are shown in Fig.8 (B).

260  
261 In ANN, ANFIS and SVM modeling processes, large attribute values might cause numerical  
262 problems because the neurons in ANN and ANFIS are combined Sigmoid function as excitation  
263 function, and the kernel values in SVM usually depend on the inner products of feature vectors,  
264 such as the linear kernel and the polynomial kernel. There are two main advantages to normalize

265 features before applying ANN, ANFIS and SVM to prediction. One advantage is to avoid  
266 attributes in greater numeric ranges dominating those in smaller numeric ranges, and another  
267 advantage is to avoid numerical difficulties during the calculation. It is recommended to linearly  
268 scale each attribute to the range [-1, +1] or [0, 1]. In the modeling process, the data sets of river  
269 flow were scaled to the range between 0 and 1 as follow:

$$270 \quad q'_i = \frac{q_i - q_{\min}}{q_{\max} - q_{\min}} \quad (12)$$

271 where  $q'_i$  is the scaled value,  $q_i$  is the original flow value and  $q_{\min}$ ,  $q_{\max}$  are respectively  
272 the minimum and maximum of flow series.

#### 273 **4. Prediction modeling and input selection**

274 We are interested in hydrological forecasting model that predict outputs from inputs based on  
275 past records. There are no fixed rules for developing these AI techniques (ANN, ANFIS, GP,  
276 SVM), even though a general framework can be followed based on previous successful  
277 applications in engineering (Cheng et al., 2005; Lin et al., 2006; Nayak et al., 2004; Sudheer et al.,  
278 2002). The objective of studies focus on predicting discharges using antecedent values is to  
279 generalize a relationship of the following form:

$$280 \quad Y = f(X^m) \quad (13)$$

281 where  $X^m$  is a m-dimensional input vector consisting of variables  $x_1, \dots, x_i, \dots, x_m$ , and  $Y$  is the output  
282 variable. In discharge modeling, values of  $x_i$  may be flow values with different time lags and the  
283 value  $Y$  is generally the flow in the next period. Generally, the number of antecedent values  
284 included in the vector  $X^m$  is not known a priori.

285 In these AI techniques, being typical in any data-driven prediction models, the selection of  
286 appropriate model input vector would play an important role in their successful implementation  
287 since it provides the basic information about the system being modeled. The parameters  
288 determined as input variables are the numbers of flow values for finding the lags of runoff that  
289 have a significant influence on the predicted flow. These influencing values corresponding to  
290 different lags can be very well established through a statistical analysis of the data series.  
291 Statistical procedures were suggested for identifying an appropriate input vector for a model (Lin  
292 et al., 2006; Sudheer et al., 2002). In this study, two statistical methods (i.e. the autocorrelation  
293 function (ACF) and the partial autocorrelation function (PACF)) are employed to determine the  
294 number of parameters corresponding to different antecedents values. The influencing antecedent  
295 discharge patterns can be suggested by the ACF and PACF in the flow at a given time. The ACF  
296 and PACF are generally used in diagnosing the order of the autoregressive process and can also be  
297 employed in prediction modeling (Lin et al., 2006). The values of ACF and PACF of monthly flow  
298 sequence (1953/1~1999/12) is calculated for lag 0 to 24 in Manwan, which are presented in Fig.10.  
299 Similarly, the values of ACF and PACF of monthly flow sequence (1951/1~1994/12) is calculated  
300 for lag 0 to 24 in Hongjiadu, which are presented in Fig.11. From Fig.10(a) and Fig.11(a), the ACF  
301 exhibits the peak at lag 12. In addition, Fig.10(b) and Fig.11(b) showed a significant correlation of  
302 PACF at 95% confidence level interval up to 12 months of flow lag. Therefore twelve antecedent  
303 flow values have the most information to predict future flow and are considered as input for



304 monthly discharge time series modeling.

## 305 **5. Model performance evaluation**

306 Some techniques are recommended for hydrological time series forecasting model performance  
 307 evaluation according to published literature related to calibration, validation, and application of  
 308 hydrological models. Four performance evaluation criteria used in this study are computed as in  
 309 the following section.

310 **The coefficient of correlation (R) or its square, the coefficient of determination (R<sup>2</sup>):** It  
 311 describes the degree of collinearity between simulated and measured data, which ranges from -1 to  
 312 1, is an index of the degree of linear relationship between observed and simulated data. If R =0, no  
 313 linear relationship exists. If R=1 or -1, a perfect positive or negative linear relationship exists. Its  
 314 equation is

$$315 \quad R = \frac{\frac{1}{n} \sum_{i=1}^n (Q_0(i) - \bar{Q}_0)(Q_f(i) - \bar{Q}_f)}{\sqrt{\frac{1}{n} \sum_{i=1}^n (Q_0(i) - \bar{Q}_0)^2} * \sqrt{\frac{1}{n} \sum_{i=1}^n (Q_f(i) - \bar{Q}_f)^2}} \quad (14)$$

316 R and R<sup>2</sup> have been widely used for model evaluation (Lin et al., 2006; Santhi et al., 2001; Van  
 317 Liew et al., 2003), though they are oversensitive to high extreme values (outliers) and insensitive  
 318 to additive and proportional differences between model predictions and measured data (Legates  
 319 and McCabe, 1999).

320 **Nash-Sutcliffe efficiency coefficient (E):** The Nash-Sutcliffe model efficiency coefficient is used  
 321 to assess the predictive power of hydrological models (Nash and Sutcliffe, 1970). It is a  
 322 normalized statistic that determines the relative magnitude of the residual variance (“noise”)  
 323 compared to the measured data variance and indicates how well the plot of observed versus  
 324 simulated data fits the 1:1 line (Moriassi et al., 2007). It is defined as:

$$325 \quad E = 1 - \frac{\sum_{i=1}^n (Q_0(i) - Q_f(i))^2}{\sum_{i=1}^n (Q_0(i) - \bar{Q}_0)^2} \quad (15)$$

326 Nash-Sutcliffe efficiencies ranges between (-∞, 1]: E=1 corresponds to a perfect match of  
 327 forecasting discharge to the observed data; E=0 shows that the model predictions are as accurate  
 328 as the mean of the observed data; and -∞<E<0 occurs when the observed mean is a better predictor  
 329 than the model, which indicates unacceptable performance.

330 **Root mean squared error (RMSE):** It is an often used measure of the difference between values  
 331 predicted by a model and those actually observed from the thing being modeled. RMSE is one of  
 332 the commonly used error index statistics (Lin et al., 2006; Nayak et al., 2004) and is defined as:

$$333 \quad RMSE = \sqrt{\frac{1}{n} \sum_{i=1}^n (Q_f(i) - Q_0(i))^2} \quad (16)$$

334 **Mean absolute percentage error (MAPE):** The MAPE is computed through a term-by-term  
 335 comparison of the relative error in the prediction with respect to the actual value of the variable.

336 Thus, the MAPE is an unbiased statistic for measuring the predictive capability of a model. It is a  
337 measure of the accuracy in a fitted time series value in statistics and has been used for river flow  
338 time series prediction evaluation (Hu et al., 2001). It usually expresses accuracy as a percentage  
339 and is defined as:

340

$$341 \quad MAPE = \frac{1}{n} \sum_{i=1}^n \left| \frac{Q_f(i) - Q_0(i)}{Q_0(i)} \right| \times 100 \quad (17)$$

342 where  $Q_0(i)$  and  $Q_f(i)$  are, respectively, the observed and forecasted discharge and  $\overline{Q_0}, \overline{Q_f}$   
343 denote their means, and n is the number data points considered.

## 344 **5. Development of models**

345 ARMA model uses the direct dependence of the previous measurements and depends on the  
346 previous innovation of the process in a moving average form. The monthly discharge series, which  
347 do fit a normal distribution with respect to the skewness coefficient, can be normalized using a  
348 log-transformation function in order to remove the periodicity in the original record (Keskin et al.,  
349 2006). In order to choose the appropriate ARMA (p, q) model, the Akaike information criteria  
350 (AIC) are used to select the value of p and q, which represent respectively the number of  
351 autoregressive orders and the number of moving-average orders of the ARMA model. In this study,  
352 the models ARMA (5, 8), (6, 7), (8, 7), (9, 8) and (11, 8), have a relatively minimum AIC value  
353 based on flow series in Manwan, and the models ARMA (5, 9), (6, 10), (7, 9), (8, 9) and (10, 11)  
354 have a relatively minimum AIC value based on flow series in Hongjiadu. Table 1 and Table 2,  
355 respectively, show their AIC values and the performance of alternative ARMA models. Hence,  
356 according to their performance indices, ARMA (8, 7) is selected as the ARMA model in Mamwan,  
357 and ARMA (6, 10) is selected as the ARMA model in Hongjiadu.

358 In this study, a typical three-layer feed-forward ANN model (Fig. 1) with a back-propagation  
359 algorithm is constructed for forecasting monthly discharge time series. The back-propagation  
360 training algorithm is a supervised training mechanism and is normally adopted in most of the  
361 engineering application. The primary goal is to minimize the error at the output layer by searching  
362 for a set of connection strengths that cause the ANN to produce outputs that are equal to or closer  
363 to the targets. The neurons of hidden layer use the tan-sigmoid transfer function, and the linear  
364 transfer function for output layer. A scaled conjugate gradient algorithm (Moller, 1993) is  
365 employed for training, and the training epoch is set to 500. The optimal number of neuron in the  
366 hidden layer was identified using a trial and error procedure by varying the number of hidden  
367 neurons from 2 to 13. The number of hidden neurons was selected based on the RMSE. The effect  
368 of changing the number of hidden neurons on the RMSE of the data set is shown in Fig. 12 and  
369 Fig. 13. It can be observed that the effect of the number of neurons assigned to the hidden layer  
370 has insignificant effect on the performance of the feed forward model. The numbers of hidden  
371 neurons were found to be four and four for Manwan and Hongjiadu, respectively.

372 The ANFIS applies a hybrid learning algorithm that combines the backpropagation gradient  
373 descent and the least squares estimate method, which outperforms the original backpropagation  
374 algorithm. An essential part of fuzzy logic is fuzzy sets defined by membership functions and rule  
375 bases. Shapes of the fuzzy sets are defined by the membership functions. The adjustment of

376 adequate membership function parameters is facilitated by a gradient vector. After determining a  
377 gradient vector, the parameters are adjusted and the performance function is minimised via  
378 least-squares estimation. For the proposed Sugeno-type model, the overall output is expressed as  
379 linear combinations of the resulting parameters. The output  $f$  in Fig. 3 can be rewritten as:

$$380 \quad f = \overline{w_1}f_1 + \overline{w_2}f_2 = (\overline{w_1x})p_1 + (\overline{w_1y})q_1 + (\overline{w_1})r_1 + (\overline{w_2x})p_2 + (\overline{w_2y})q_2 + (\overline{w_2})r_2 \quad (18)$$

381 The resulting parameters ( $p_1, q_1, r_1, p_2, q_2, r_2$ ) are computed by the least-squares method.  
382 Consequently, the optimal parameters of the ANFIS model can be estimated using the hybrid  
383 learning algorithm. For more detail, please refer to Jang and Sun (Jang et al., 1997).

384 GP has the ability to generate the best computer program to describe the relationship between  
385 the input and output. In this study, in order to find the optimal monthly flow series forecasting  
386 model, the selection of the appropriate parameters of GP evolution is necessary. Although the  
387 fine-tuning of algorithm was not the main concern of this paper, we investigated various  
388 initialization and run approaches and the adopted GP parameters are presented in Table 3. This  
389 setup furnished stable and effective runs throughout experiments. The evolutionary procedures are  
390 similar to GAs including defining the fitness function, genetic operators such as crossover,  
391 mutation and reproduction and the termination criterion, etc. In GP, the crossover operator is used  
392 to swap the subtree from the parents to reproduce the children using mating selection policy rather  
393 than exchanging bit strings as in GAs.

394 A kernel function has to be selected from the qualified functions in using SVM. Dibike et al.  
395 (2001) applied different kernels in SVR to rainfall- runoff modeling and demonstrated that the  
396 radial basis function (RBF) outperforms other kernel functions. Also, many works on the use of  
397 SVR in hydrological modeling and forecasting have demonstrated the favorable performance of  
398 the RBF (Khan and Coulibaly, 2006; Lin et al., 2006; Liong and Sivapragasam, 2002; Yu et al.,  
399 2006). Therefore, the RBF is used as the kernel function for prediction of discharge in this study.  
400 There are three parameters in using RBF kernels:  $C$ ,  $\varepsilon$  and  $\sigma$ . the accuracy of a SVM model is  
401 largely dependent on the selection of the model parameters. However, structured methods for  
402 selecting parameters are lacking. Consequently, some kind of model parameter calibration should  
403 be made. Recently, there are several methods developed to identify the parameters, such as the  
404 simulated annealing algorithms (Pai and Hong, 2005), GA (Pai, 2006) and the shuffled complex  
405 evolution algorithm (SCE-UA) (Lin et al., 2006; Yu et al., 2004). The SCE-UA method belongs to  
406 the family of evolution algorithm and was presented by Duan et al. (1993). In this study, the  
407 SCE-UA is employed as the method of optimizing parameters of SVM and a more comprehensive  
408 presentation can be found by Lin et al. (2006). To reach at a suitable choice of these parameters,  
409 the RMSE was used to optimize the parameters. Optimal parameters ( $C, \varepsilon, \sigma$ ) = (19.9373,  
410 8.7775e-004, 1.2408) and ( $C, \varepsilon, \sigma$ ) = (0.5045, 5.0814e-004, 0.6623) were obtained for Manwan  
411 and Hongjiadu, respectively.

## 412 **6. Results and discussion**

413 The Manwan Hydropower, has been studied by Cheng et al. (2005) using ANFIS with  
414 discharges of monthly river flow discharges during 1953-2003, and by Lin et al. (2006) using  
415 SVM with discharges of monthly river flow discharges during 1974-2003. In their study, the R and  
416 RMSE were employed for evaluation model performance. In this paper, in order to identify more

417 suitable models for forecasting future monthly inflows to hydropower reservoirs, the monthly  
418 discharge time series data of two study sites in different rivers are applied. For the same basis of  
419 comparison, the same training and verification sets, respectively, are used for all the above models  
420 developed, whilst the four quantitative standard statistical performance evaluation measures are  
421 employed to evaluate the performances of various models developed. Tables 4 and 5 present the  
422 results of Manwan and Hongjiadu study sites respectively, in terms of various performance  
423 statistics

424 It can be observed from Tables 4 and 5 that various AI methods have good performance during  
425 both training and validation, and they outperform ARMA in terms of all the standard statistical  
426 measures. For Manwan hydropower, in the training phase, the ANFIS model obtained the best R,  
427 RMSE, and E statistics of 0.932, 329.77, and 0.869, respectively; while the SVM model obtained  
428 the best MAPE statistics of 12.49. Analyzing the results during testing, it can be observed that the  
429 SVM model outperforms all other models. Similarly, for Hongjiadu hydropower, in the training  
430 phase, the ANFIS model obtained the best RMSE and E statistics of 887.38 and 0.564,  
431 respectively; while the SVM model obtained the best R and MAPE statistics of 0.753 and 28.25,  
432 respectively. Analyzing the results during testing, the SVM model obtained the best R and MAPE  
433 statistics of 0.823 and 33.77, respectively; while the GP model obtained the best RMSE, and E  
434 statistics of 86.07 and 0.654, respectively. RMSE evaluates the residual between observed and  
435 forecasted flow, and MAPE measures the mean absolute percentage error of the forecast. R  
436 evaluates the linear correlation between the observed and computed flow, while E evaluates the  
437 capability of the model in predicting flow values away from the mean. According to the figures in  
438 Tables 4 and 5, we can conclude that the best performance of all AI methods developed in this  
439 paper is different in terms of the different statistical measures.

440 In addition, in the validation phase as seen in Tables 4 and 5, the values with the ANFIS, GP and  
441 SVM model prediction were able to produce a good, near forecast, as compared to those with  
442 ARMA and ANN model, whilst it can be concluded that the ANFIS model obtained the best  
443 minimum absolute error between the observed and modeled maximum and minimum peak flows  
444 in Manwan Hydropower, and the GP and SVM model obtained the best minimum absolute error  
445 between the observed and modeled maximum and minimum peak flows, respectively, in  
446 Hongjiadu Hydropower. In the validation phase, the SVM model improved the ARMA forecast of  
447 about 6.06% and 20.12% reduction in RMSE and MAPE values, respectively; Improvements of  
448 the forecast results regarding the R and E were approximately 1.22% and 1.69%, respectively in  
449 Manwan Hydropower. In Hongjiadu Hydropower, the GP model obtained the best value of RMSE  
450 during the validation phase decreases by 8.77% and the best value of E increases by 11.99%  
451 comparing with ARMA; while, the SVM model obtained the best value of R during the validation  
452 phase increases by 4.71% and the best value of MAPE decreases by 29.69% comparing with  
453 ARMA. Thus the results of this analysis indicate that the ANFIS or SVM is able to obtain the best  
454 result in terms of different evaluation measures during the training phase, and the GP or SVM is  
455 able to obtain the best result in terms of different evaluation measures during the validation phase.  
456 Furthermore, as can be seen from Tables 4 and 5 that the virtues or defect degree of forecasting  
457 accuracy is different in terms of different evaluation measures during the training phase and the  
458 validation phase. SVM model is able to obtain the better forecasting accuracy in terms of different  
459 evaluation measures during the validation phase not only during the training phase but also during  
460 the validation phase. The forecasting results of ANFIS model during the validation phase are

461 inferior to the results during the training phase. GP is in the middle or lower level in training  
462 phases, but the GP model is able to obtain the better forecasting result in validation phases, and  
463 especially the GP model is able to obtain the maximum peak flows among all models developed in  
464 Hongjiadu Hydropower. The performances of all prediction models developed in this paper during  
465 the training and validation periods in the two study sites are shown in Fig. 14 to 17.

## 466 **7. Conclusions**

467 An attempt was made in this study to investigate the performance of several AI methods for  
468 forecasting monthly discharge time series. The forecasting methods investigated include the ANNs  
469 ANFIS techniques, GP models and SVM method. The conventional ARMA is also employed as a  
470 benchmarking yardstick for comparison purposes. The monthly discharge data from actual field  
471 observed data in the Manwan Hydropower and Hongjiadu Hydropower were employed to develop  
472 various models investigated in this study. The methods utilize the statistical properties of the data  
473 series with certain amount of lagged input variables. Four standard statistical performance  
474 evaluation measures are adopted to evaluate the performances of various models developed.

475 The results obtained in this study indicate that the AI methods are powerful tools to model the  
476 discharge time series and can give good prediction performance than traditional time series  
477 approaches. The results indicate that the best performance can be obtained by ANFIS, GP and  
478 SVM, in terms of different evaluation criteria during the training and validation phases. SVM  
479 model is able to obtain the better forecasting accuracy in terms of different evaluation measures  
480 during the validation phase during both the training phase and the validation phase. The  
481 forecasting results of ANFIS model during the validation phase are inferior to the results during  
482 the training phase. GP is in the middle or lower level in training phases, but the GP model is able  
483 to obtain the better forecasting result in validation phases. The ANFIS and GP model obtain the  
484 maximum peak flows among all models developed in different studies sites, respectively.  
485 Therefore, the results of the study are highly encouraging and suggest that ANFIS, GP and SVM  
486 approaches are promising in modeling monthly discharge time series, and this may provide  
487 valuable reference for researchers and engineers who apply AI methods for modeling long-term  
488 hydrological time series forecasting. It is hoped that future research efforts will focus in these  
489 directions, i.e. more efficient approach for training multi-layer perceptrons of ANN model, the  
490 increased learning ability of the ANFIS model, the fine-tuning of algorithm for selecting more  
491 appropriate parameters of GP evolution, saving computing time or more efficient optimization  
492 algorithms in searching optimal parameters of SVM model etc to improve the accuracy of the  
493 forecast models in terms of different evaluation measures for better planning, design, operation,  
494 and management of various engineering systems.

## 495 **Acknowledgements**

496 This research was supported by the Central Research Grant of Hong Kong Polytechnic University  
497 (G-U265), the National Natural Science Foundation of China (No.50679011), Doctor Foundation  
498 of higher education institutions of China (No.20050141008).

499 **Reference**

- 500 ASCE Task Committee., 2000a. Artificial neural networks in hydrology-I: Preliminary concepts.  
501 *Journal of Hydrologic Engineering*, ASCE 5(2): 115-123.
- 502 ASCE Task Committee., 2000b. Artificial neural networks in hydrology-II: Hydrological  
503 applications. *Journal of Hydrologic Engineering*, ASCE5(2): 124-137.
- 504 Asefa, T., Kemblowski, M., McKee, M. and Khalil, A., 2006. Multi-time scale stream flow  
505 predictions: The support vector machines approach. *Journal of Hydrology*, 318(1-4): 7-16.
- 506 Bazartseren, B., Hildebrandt, G. and Holz, K.P., 2003. Short-term water level prediction using  
507 neural networks and neuro-fuzzy approach. *Neurocomputing*, 55(3-4): 439-450.
- 508 Borrelli, A., De Falco, I., Della Cioppa, A., Nicodemi, M. and Trautteur, G., 2006. Performance of  
509 genetic programming to extract the trend in noisy data series. *Physica a-Statistical  
510 Mechanics and Its Applications*, 370(1): 104-108.
- 511 Box, G.E.P. and Jenkins, G.M., 1970. *Times series Analysis Forecasting and Control*. Holden-Day,  
512 San Francisco.
- 513 Campolo, M., Soldati, A. and Andreussi, P., 2003. Artificial neural network approach to flood  
514 forecasting in the River Arno. *Hydrological Sciences Journal*, 48(3): 381-398.
- 515 Chang, L.C. and Chang, F.J., 2001. Intelligent control for modelling of real-time reservoir  
516 operation. *Hydrological Processes*, 15(9): 1621-1634.
- 517 Chau, K.W., 2006. Particle swarm optimization training algorithm for ANNs in stage prediction of  
518 Shing Mun River. *Journal of Hydrology*, 329(3-4): 363-367.
- 519 Chau, K.W. and Cheng, C.T., 2002. Real-time prediction of water stage with artificial neural  
520 network approach. *Lecture Notes in Artificial Intelligence*, 2557: 715.
- 521 Chen, H.L. and Rao, A.R., 2002. Testing hydrologic time series for stationarity. *Journal of  
522 Hydrologic Engineering*, 7(2): 129-136.
- 523 Cheng, C.T., Lin, J.Y., Sun, Y.G. and Chau, K.W., 2005. Long-term prediction of discharges in  
524 Manwan hydropower using adaptive-network-based fuzzy inference systems models,  
525 *Advances in Natural Computation*, Pt 3, Proceedings. *Lecture Notes in Computer Science*.  
526 Springer-Verlag Berlin, Berlin, pp. 1152-1161.
- 527 Dibike, Y.B., Velickov, S., Solomatine, D. and Abbott, M.B., 2001. Model induction with support  
528 vector machines: Introduction and applications. *Journal of Computing in Civil  
529 Engineering*, 15(3): 208-216.
- 530 Dixon, B., 2005. Applicability of neuro-fuzzy techniques in predicting ground-water vulnerability:  
531 a GIS-based sensitivity analysis. *Journal of Hydrology*, 309(1-4): 17-38.
- 532 Duan, Q.Y., Gupta, V.K. and Sorooshian, S., 1993. Shuffled complex evolution approach for  
533 effective and efficient minimization. *Journal of Optimization Theory and Applications*,  
534 76(3): 501-521.
- 535 Haykin, S., 1999. *Neural networks: a comprehensive foundation*. 2nd ed. Upper Saddle River,  
536 New Jersey.
- 537 Hu, T.S., Lam, K.C. and Ng, S.T., 2001. River flow time series prediction with a range-dependent  
538 neural network. *Hydrological Sciences Journal*, 46(5): 729-745.
- 539 Jang, J.-S.R., 1993. ANFIS: Adaptive-Network-based Fuzzy Inference Systems. *IEEE  
540 Transactions on Systems, Man, and Cybernetics*, 23(3): 665-685.
- 541 Jang, J.-S.R., Sun, C.-T. and Mizutani, E., 1997. *Neuro-Fuzzy and Soft Computing: A*

- 542 Computational Approach to Learning and Machine Intelligence. Prentice-Hall, Upper  
543 Saddle River, NJ.
- 544 Johari, A., Habibagahi, G. and Ghahramani, A., 2006. Prediction of soil-water characteristic curve  
545 using genetic programming. *Journal of Geotechnical and Geoenvironmental Engineering*,  
546 132(5): 661-665.
- 547 Keskin, M.E., Taylan, D. and Terzi, O., 2006. Adaptive neural-based fuzzy inference system  
548 (ANFIS) approach for modelling hydrological time series. *Hydrological Sciences Journal*,  
549 51(4): 588-598.
- 550 Khan, M.S. and Coulibaly, P., 2006. Application of support vector machine in lake water level  
551 prediction. *Journal of Hydrologic Engineering*, 11(3): 199-205.
- 552 Koza, J., 1992. *Genetic Programming: On the Programming of Computers by Natural Selection*.  
553 MIT Press, Cambridge, MA.
- 554 Legates, D.R. and McCabe, G.J., 1999. Evaluating the use of "goodness-of-fit" measures in  
555 hydrologic and hydroclimatic model validation. *Water Resources Research*, 35(1):  
556 233-241.
- 557 Lin, J.Y., Cheng, C.T. and Chau, K.W., 2006. Using support vector machines for long-term  
558 discharge prediction. *Hydrological Sciences Journal*, 51(4): 599-612.
- 559 Liong, S.Y. et al., 2002. Genetic Programming: A new paradigm in rainfall runoff modeling.  
560 *Journal of the American Water Resources Association*, 38(3): 705-718.
- 561 Liong, S.Y. and Sivapragasam, C., 2002. Flood stage forecasting with support vector machines.  
562 *Journal of the American Water Resources Association*, 38(1): 173-186.
- 563 Moller, M.F., 1993. A scaled conjugate gradient algorithm for fast supervised learning. *Neural*  
564 *Networks*, 6(4): 525-533.
- 565 Moriasi, D.N. et al., 2007. Model evaluation guidelines for systematic quantification of accuracy  
566 in watershed simulations. *Transactions of the ASABE*, 50(3): 885-900.
- 567 Muttill, N. and Chau, K.W., 2006. Neural network and genetic programming for modelling coastal  
568 algal blooms. *International Journal of Environment and Pollution*, 28(3-4): 223-238.
- 569 Nash, J.E. and Sutcliffe, J.V., 1970. River flow forecasting through conceptual models part I — A  
570 discussion of principles. *Journal of Hydrology*, 10(3): 282-290.
- 571 Nayak, P.C., Sudheer, K.P., Rangan, D.M. and Ramasastri, K.S., 2004. A neuro-fuzzy computing  
572 technique for modeling hydrological time series. *Journal of Hydrology*, 291(1-2): 52-66.
- 573 Pai, P.-F., 2006. System reliability forecasting by support vector machines with genetic algorithms.  
574 *Mathematical and Computer Modelling*, 43(3-4): 262-274.
- 575 Pai, P.-F. and Hong, W.-C., 2005. Support vector machines with simulated annealing algorithms in  
576 electricity load forecasting. *Energy Conversion and Management*, 46(17): 2669-2688.
- 577 Salas, J.D., 1993. Analysis and modeling of hydrologic time series. In: Maidment, D.R., Editor,  
578 1993. *The McGraw Hill Handbook of Hydrology*, pp. 19.5–19.9.
- 579 Santhi, C. et al., 2001. Validation of the swat model on a large river basin with point and nonpoint  
580 sources. *Journal of the American Water Resources Association*, 37(5): 1169-1188.
- 581 Sivapragasam, C., Vincent, P. and Vasudevan, G., 2007. Genetic programming model for forecast  
582 of short and noisy data. *Hydrological Processes*, 21(2): 266-272.
- 583 Srikanthan, R. and McMahon, T.A., 2001. Stochastic generation of annual, monthly and daily  
584 climate data: A review. *Hydrology and Earth System Sciences*, 5(4): 653-670.
- 585 Sudheer, K.P., Gosain, A.K. and Ramasastri, K.S., 2002. A data-driven algorithm for constructing

- 586           artificial neural network rainfall-runoff models. *Hydrological Processes*, 16(6):  
587           1325-1330.
- 588   Van Liew, M.W., Arnold, J.G. and Garbrecht, J.D., 2003. Hydrologic simulation on agricultural  
589           watersheds: Choosing between two models. *Transactions of the Asae*, 46(6): 1539-1551.
- 590   Vapnik, V., 1995. *The Nature of Statistical Learning Theory*. Springer, New York.
- 591   Vapnik, V., 1998. *Statistical learning theory*. Wiley, New York.
- 592   Whigam, P.A. and Crapper, P.F., 2001. Modelling Rainfall-Runoff Relationships using Genetic  
593           Programming. *Mathematical and Computer Modelling* 33: 707-721.
- 594   Yu, P.S., Chen, S.T. and Chang, I.F., 2006. Support vector regression for real-time flood stage  
595           forecasting. *Journal of Hydrology*, 328(3-4): 704-716.
- 596   Yu, X.Y., Liong, S.Y. and Babovic, V., 2004. EC-SVM approach for real-time hydrologic  
597           forecasting. *Journal of Hydroinformatics*, 6(3): 209-223.
- 598
- 599



600

601 **Table.1.** AIC value and performance indices of alternative ARMA models for Manwan  
602 hydropower

(p, q)	AIC	Training				Validation			
		R	E	RMSE	MAPE	R	E	RMSE	MAPE
(5, 8)	12.043	0.916	0.839	365.60	17.56	0.927	0.878	359.22	15.72
(6, 7)	12.045	0.915	0.838	366.78	17.42	0.925	0.874	355.18	15.56
(8, 7)	11.786	0.922	0.849	354.27	16.77	0.928	0.869	354.35	15.43
(9, 8)	11.813	0.921	0.847	356.98	16.47	0.923	0.856	380.69	15.89
(11, 8)	11.817	0.921	0.848	355.95	16.13	0.928	0.859	376.04	15.26

603

604

605 **Table.2.** AIC value and performance indices of alternative ARMA models for Hongjiadu  
606 hydropower

(p, q)	AIC	Training				Validation			
		R	E	RMSE	MAPE	R	E	RMSE	MAPE
(5,9)	9.231	0.722	0.523	91.57	44.06	0.760	0.557	97.32	49.76
<b>(6,10)</b>	9.221	0.725	0.521	91.57	46.42	0.786	0.584	94.34	48.03
(7,9)	9.242	0.724	0.520	91.89	44.91	0.748	0.538	99.39	48.50
(8,9)	9.252	0.726	0.516	92.24	45.56	0.754	0.540	99.21	47.60
(10,11)	9.268	0.722	0.501	93.68	42.30	0.760	0.540	99.22	46.29

607

608

**Table 3.** Values of primary parameters used in GP runs

Parameter	Value
Terminal set	Variable x, random (0,1)
Function set	+, -, *, /, sin, cos, ^
Population:	2000 individuals
The maximum number of generations:	100
Crossover rate:	0.9
Mutation rate:	0.05
Selection:	Tournament with elitist strategy
Initial population:	Ramped-half-and-half
The maximum depth of tree representation	9

609

610

611 **Table.4.** Forecasting performance indices of models for Manwan hydropower

Model	Training				Validation					
	R	RMSE	MAPE	E	R	RMSE	MAPE	E	Min	Max
Observed									334.0	3821.0
ARMA	0.922	354.27	16.77	0.849	0.928	354.35	15.63	0.869	373.4	3115.7
ANN	0.925	346.31	16.16	0.856	0.932	345.37	14.01	0.867	369.6	3307.8
ANFIS	<b>0.9322</b>	<b>329.77</b>	15.02	<b>0.869</b>	0.9405	335.02	14.30	0.883	<b>343.7</b>	<b>3509.3</b>
GP	0.918	360.96	17.79	0.843	0.9408	334.04	14.69	<b>0.8838</b>	360.1	3321.0
SVM	0.9315	334.07	<b>12.49</b>	0.866	<b>0.9410</b>	<b>332.86</b>	<b>12.49</b>	<b>0.8836</b>	369.0	3333.6

612 Notes: Min means minimum peak flows, and Max means maximum peak flows

613

614

615 **Table.5.** Forecasting performance indices of models for Hongjiadu hydropower

Model	Training				Validation					
	R	RMSE	MAPE	E	R	RMSE	MAPE	E	Min	Max
Observed									25.5	619.0
ARMA	0.727	91.56	46.42	0.521	0.786	94.34	48.03	0.584	11.1	357.0
ANN	0.725	91.16	46.25	0.526	0.786	91.07	46.15	0.612	39.1	358.7
ANFIS	0.751	<b>87.38</b>	47.41	<b>0.564</b>	0.801	88.71	46.67	0.632	17.8	416.9
GP	0.734	90.28	50.29	0.535	0.815	<b>86.07</b>	50.81	<b>0.654</b>	27.6	<b>430.1</b>
SVM	<b>0.753</b>	89.89	<b>28.25</b>	0.539	<b>0.823</b>	87.57	<b>33.77</b>	0.641	<b>24.6</b>	382.8

616 Notes: Min means minimum peak flows, and Max means maximum peak flows

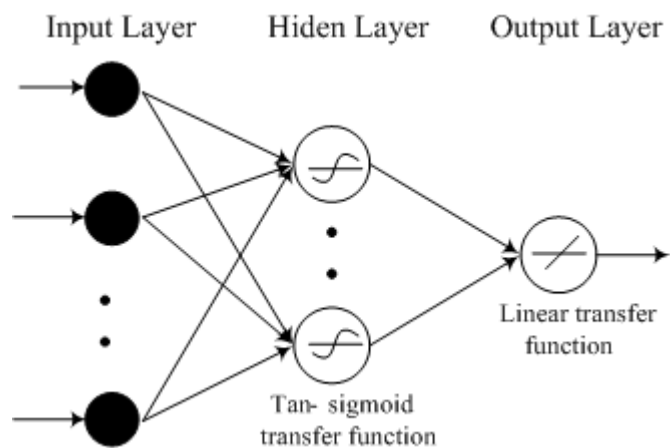
617

618

619

620 List of all figures

621



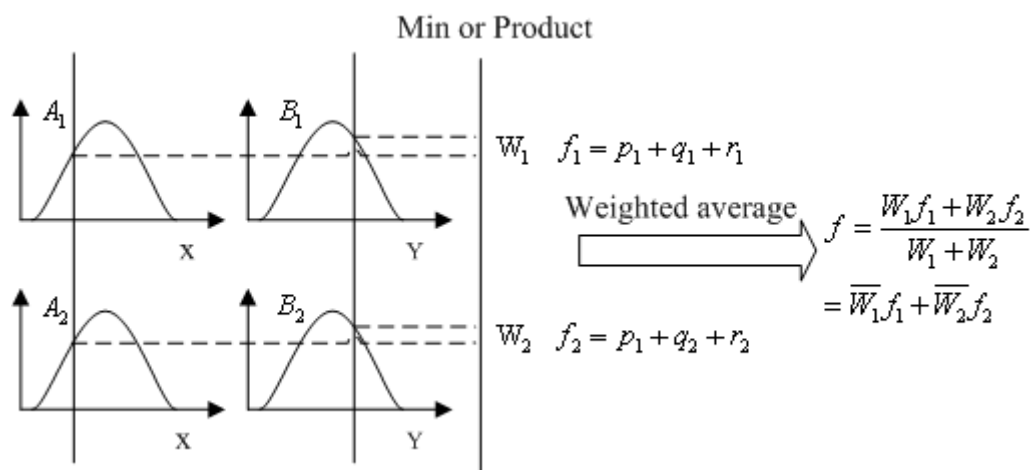
622

623

624

625

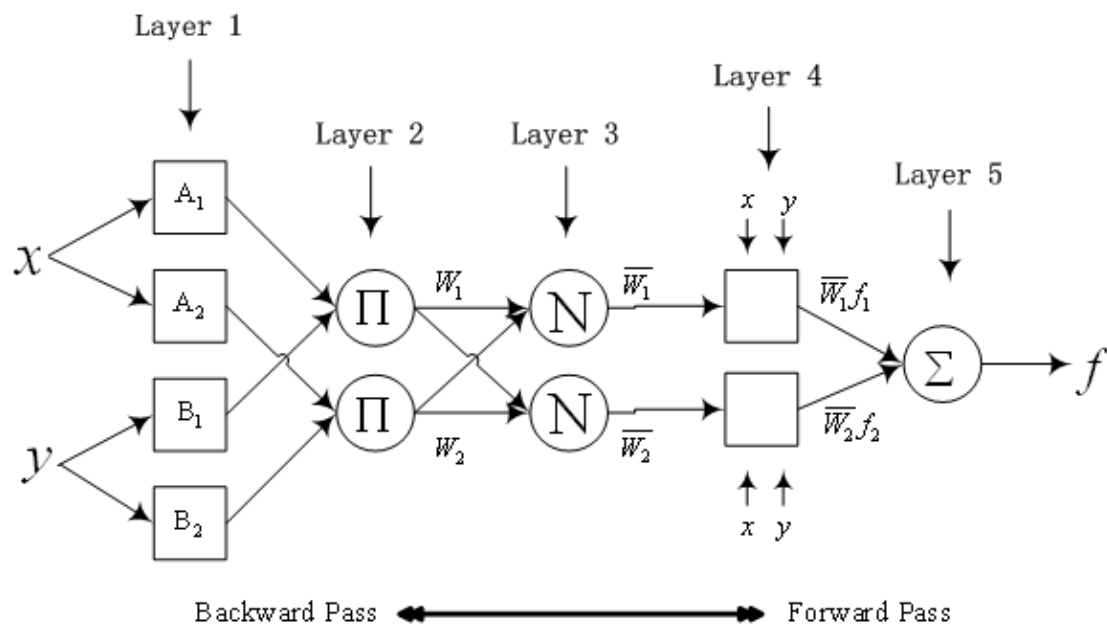
Fig.1. Architecture of three layers feed-forward back-propagation ANN



626

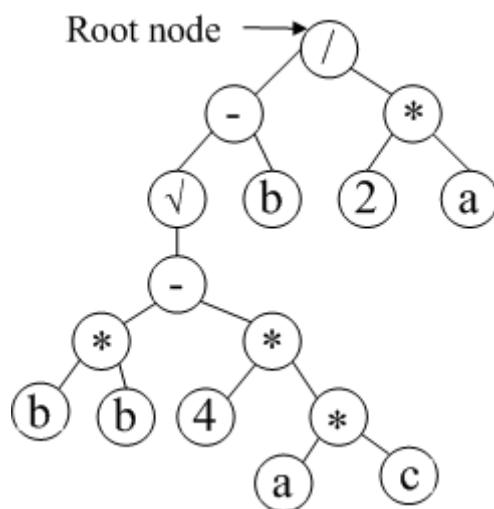
627

Fig.2. Two inputs first-order Sugeno fuzzy model with two rules



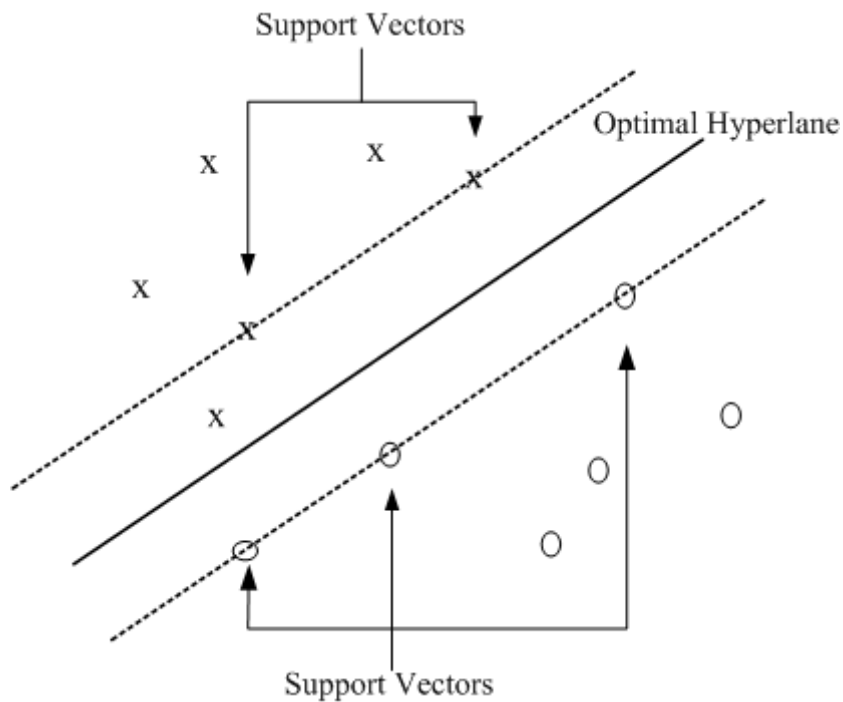
628  
629  
630  
631

Fig.3. Architecture of ANFIS



632  
633  
634

Fig. 4. GP parse tree representing function  $(\sqrt{b^2 - 4ac} - b) / 2a$

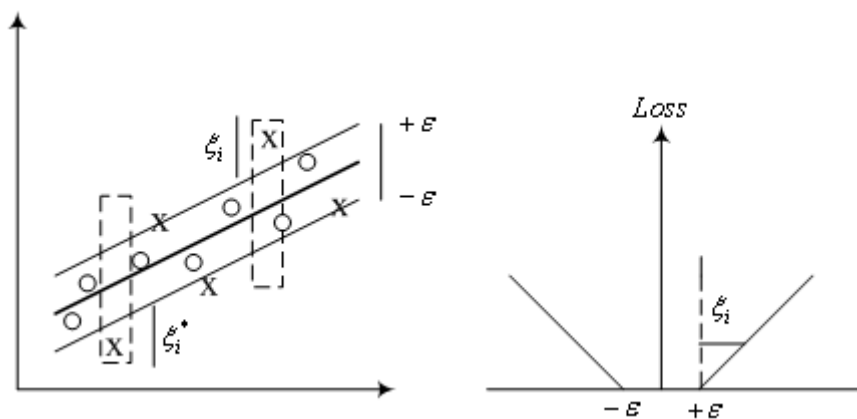


635

636

637

**Fig. 5.** The basis of the support vector machines.



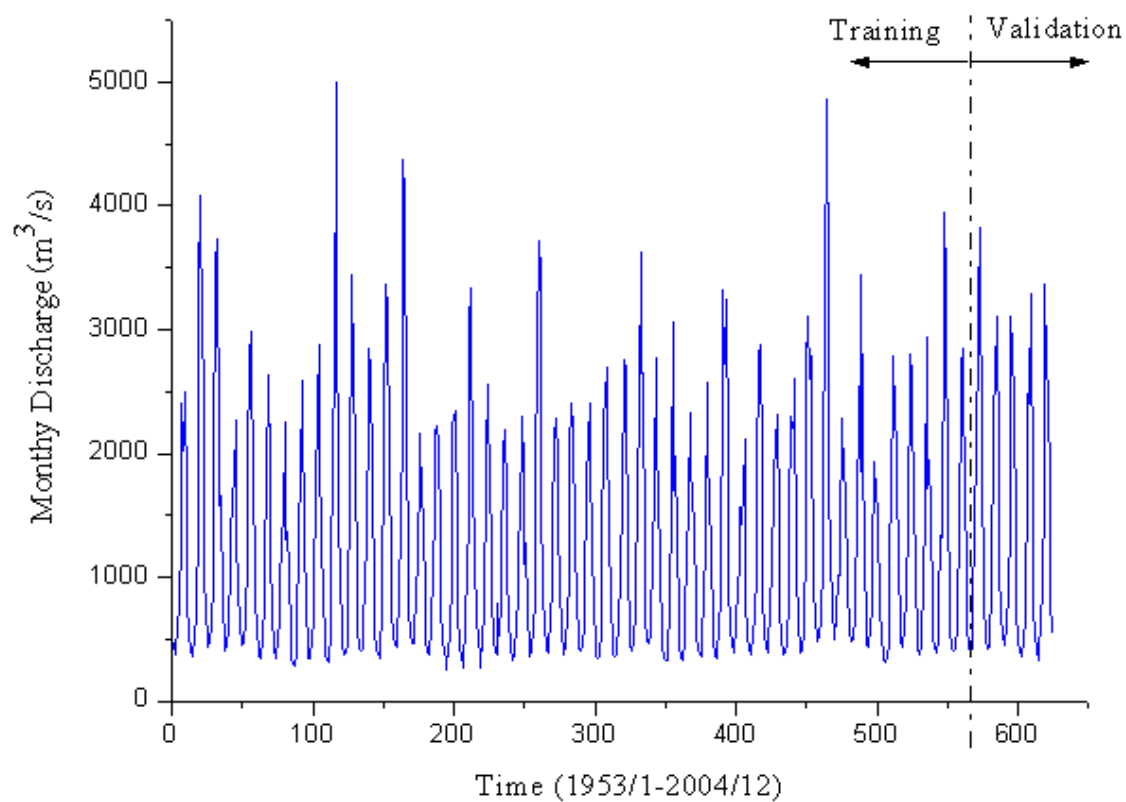
638

639

640

641

**Fig.6.** The soft margin loss setting for a linear SVM and  $\epsilon$ -insensitive loss function

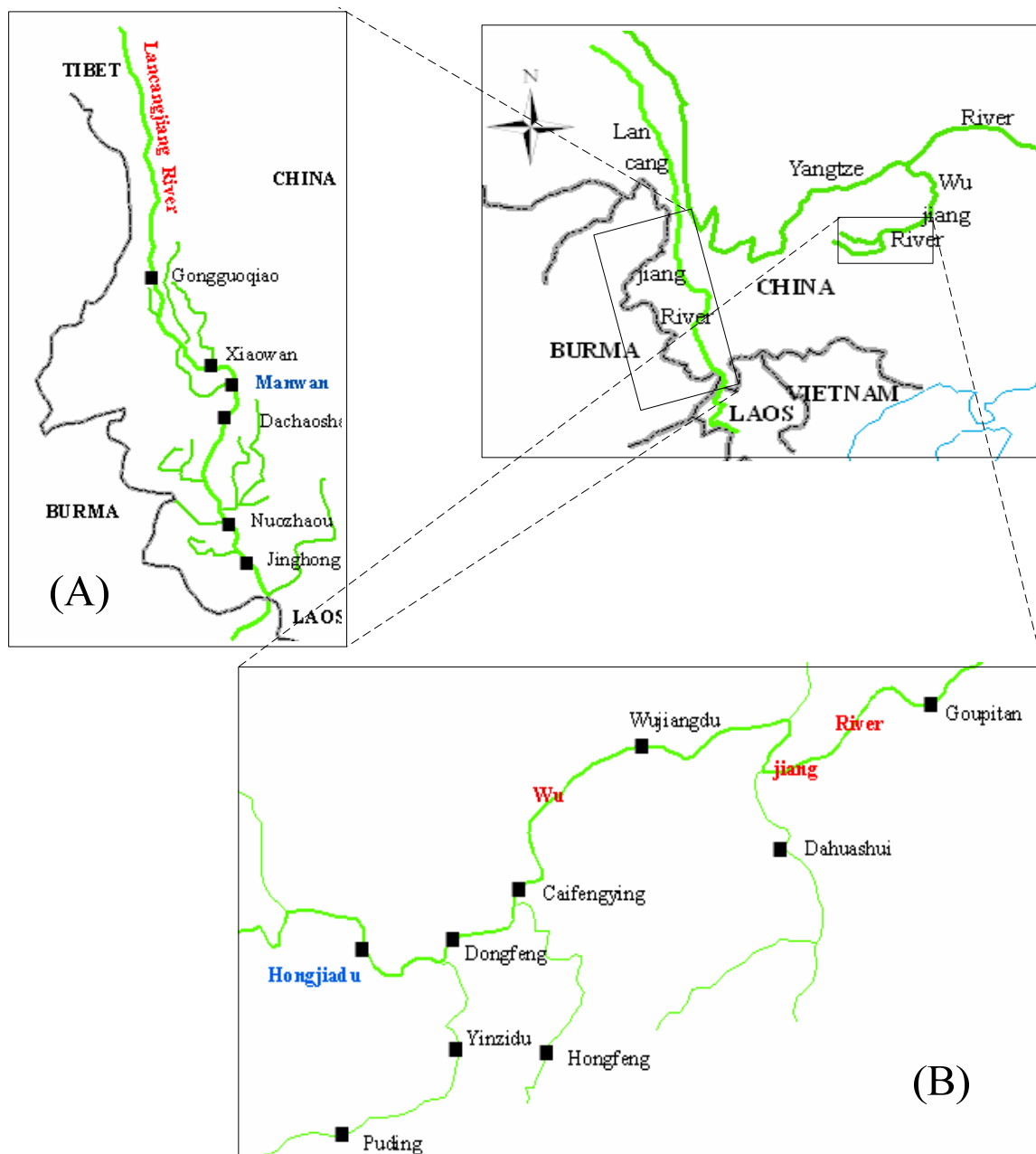


642

643

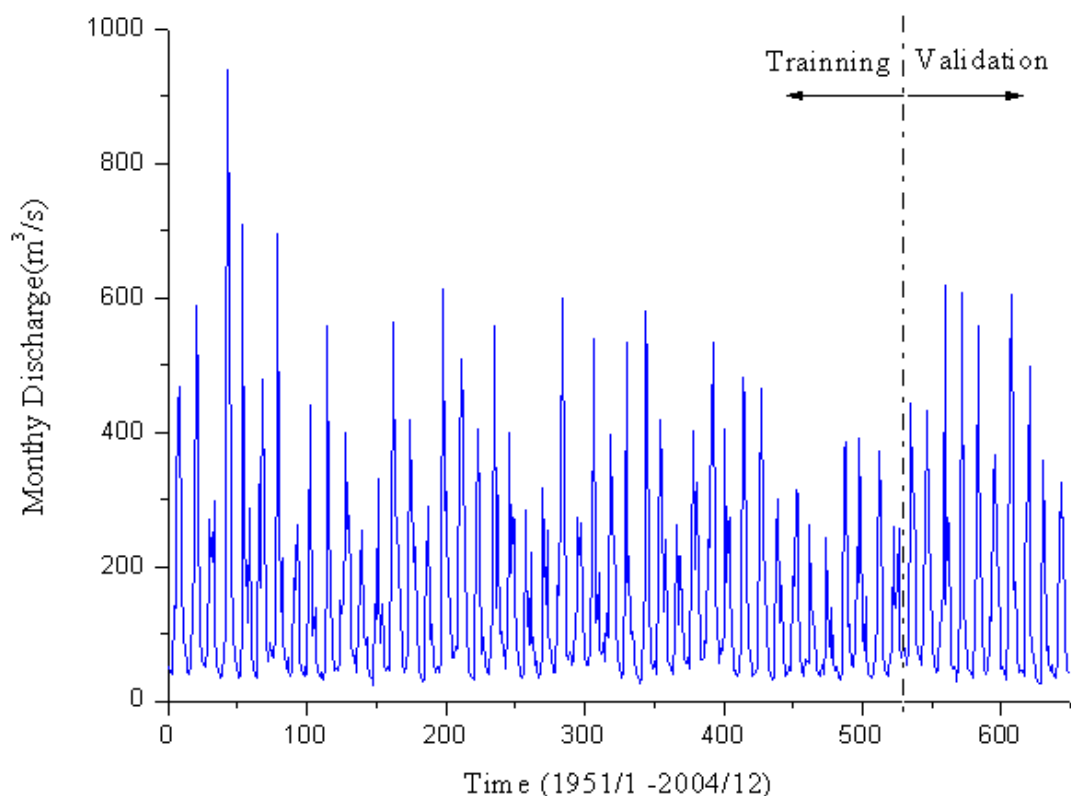
644

Fig. 7. Monthly discharge at Manwan Reservoir



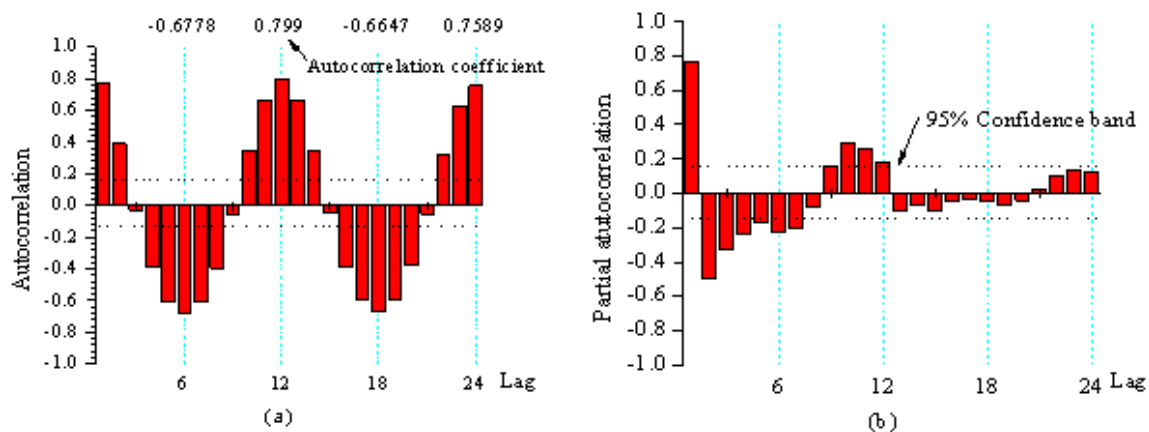
645  
646  
647  
648  
649

Fig. 8 Location of study sites



650  
651  
652

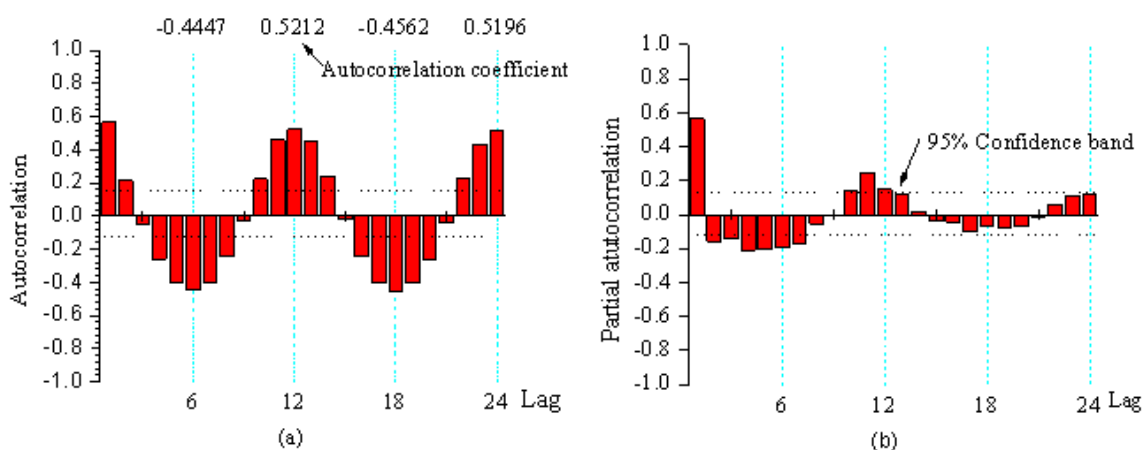
Fig. 9 Monthly discharge at Hongjiadu Reservoir



653  
654  
655  
656  
657

Fig.10. (a) the autocorrelation function of flow series. (b)The partial autocorrelation function of flow series in Manwan

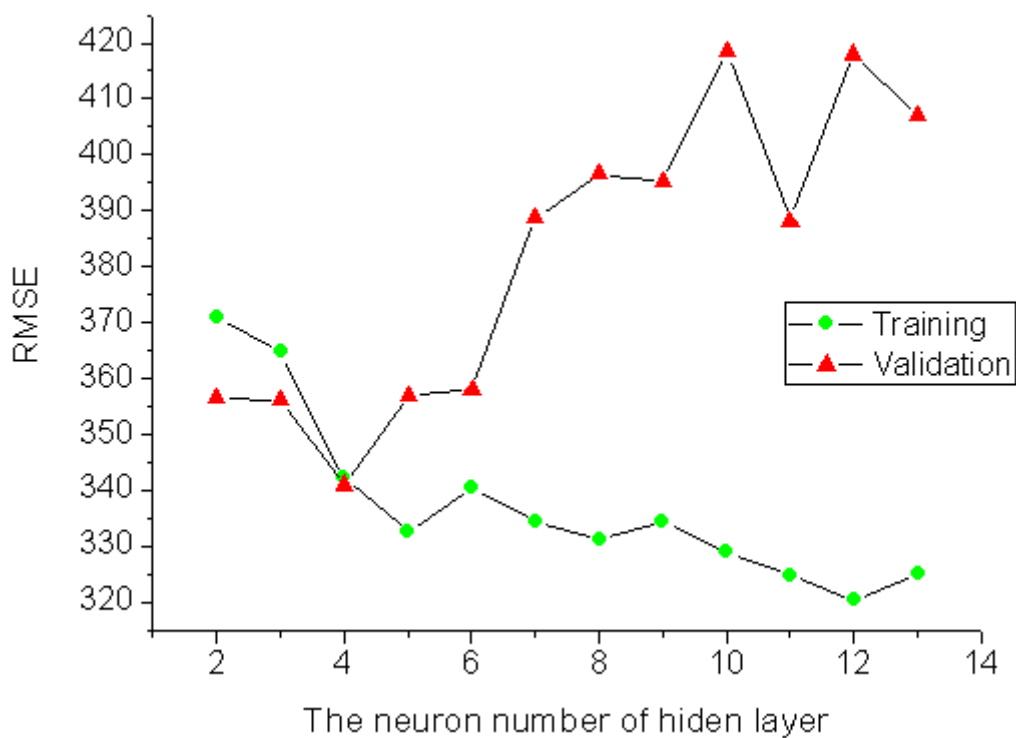




658

659 Fig.11 (a) The autocorrelation function of flow series. (b)The partial autocorrelation function of  
660 flow series in Hongjiadu.

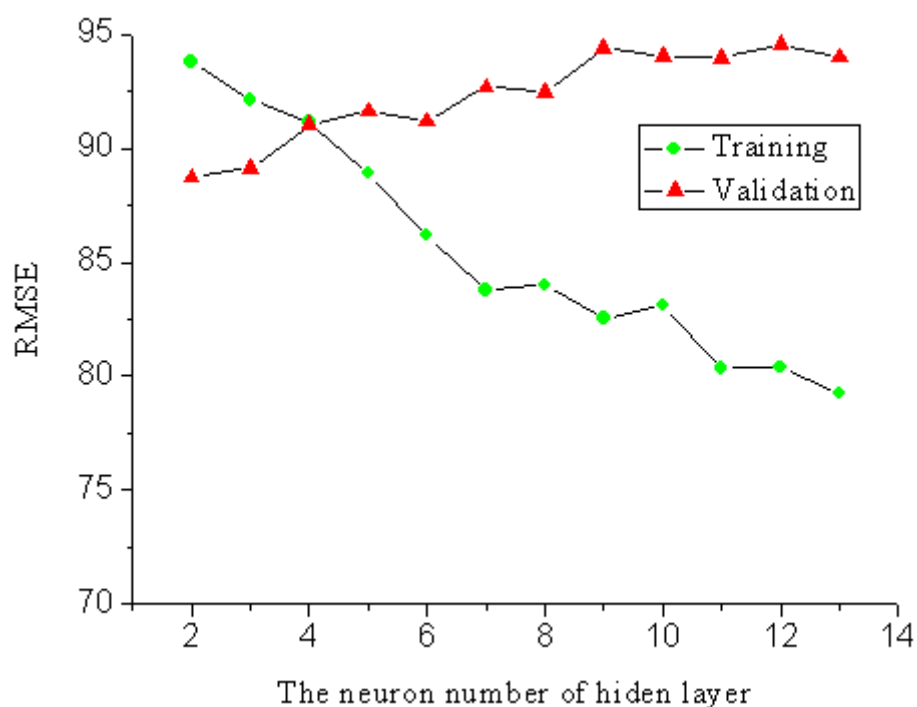
661



662

663 Fig. 12 Sensitivity of the number of nodes in the hidden layer on the RMSE of the neural network  
664 for Manwan hydropower

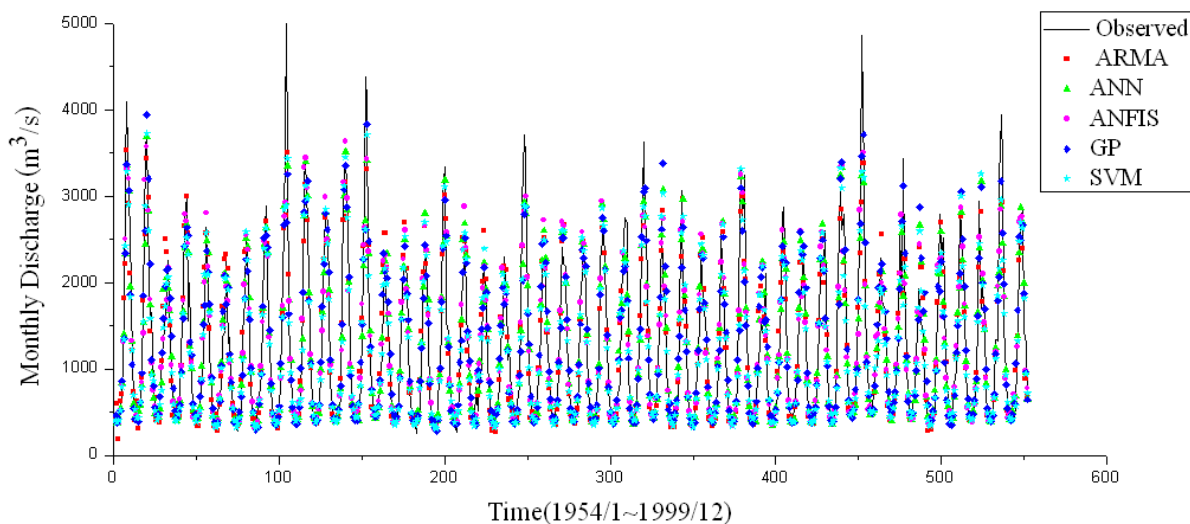
665



666

667 Fig. 13 Sensitivity of the number of nodes in the hidden layer on the RMSE of the neural network  
 668 for Hongjiadu hydropower

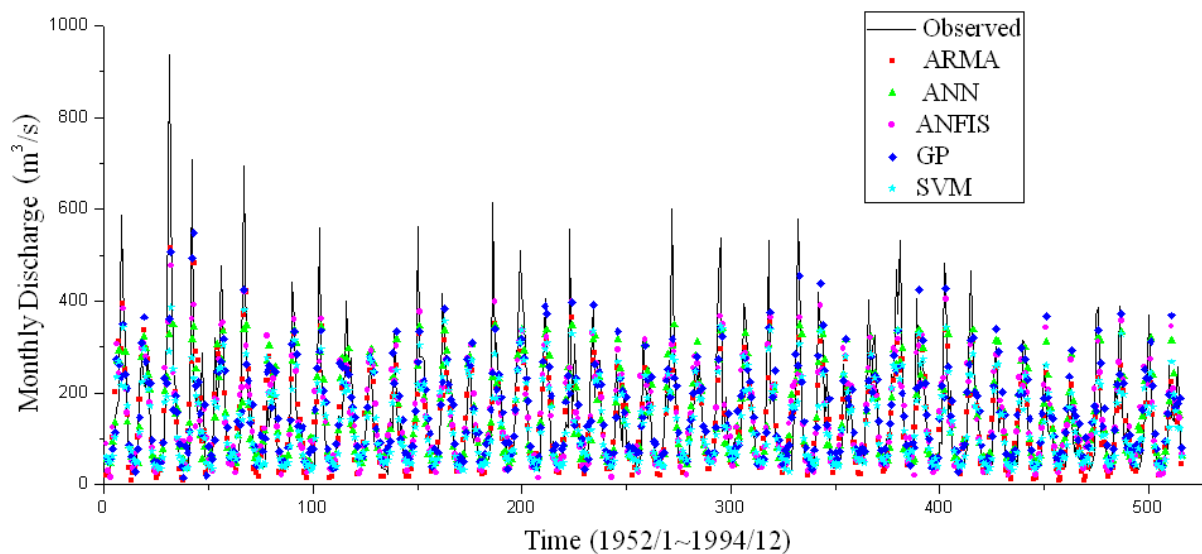
669



670

671 Fig.14 Forecasted and observed flow during training period by ARMA, ANN, ANFIS, GP and  
 672 SVM for Manwan hydropower

673

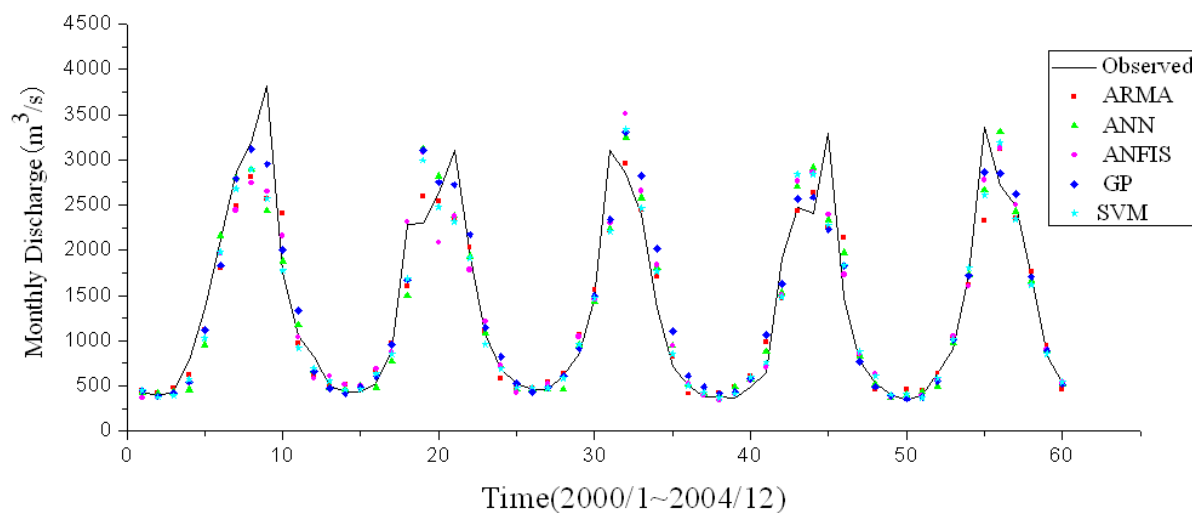


674

675 Fig.15 Forecasted and observed flow during training period by ARMA, ANN, ANFIS, GP and  
676 SVM for Hongjiadu hydropower

677

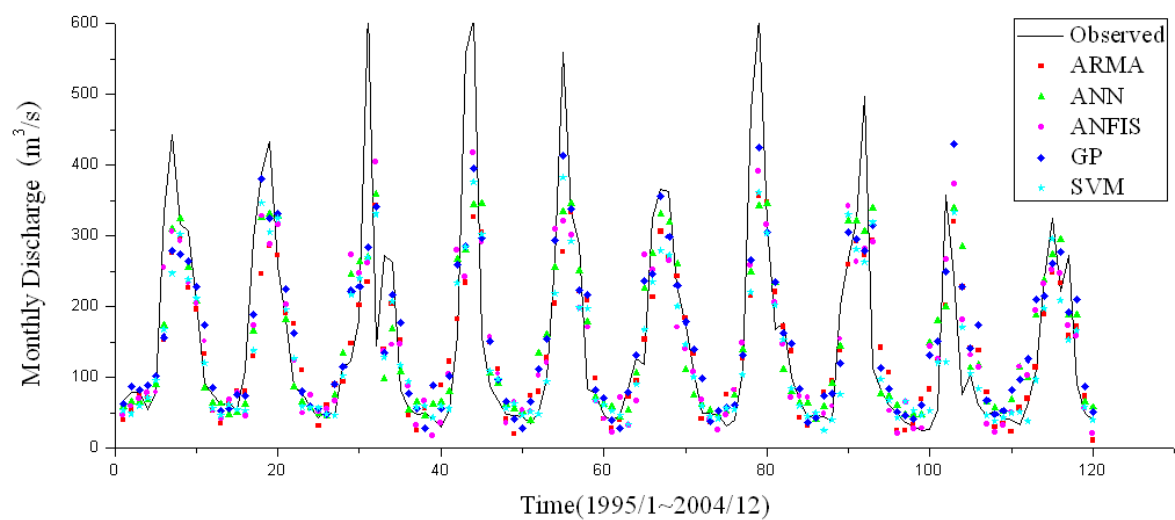
678



679

680 Fig.16 Forecasted and observed flow during validation period by ARMA, ANN, ANFIS, GP and  
681 SVM for Manwan hydropower

682



683

684

685

Fig.17 Forecasted and observed flow during validation period by ARMA, ANN, ANFIS, GP and SVM for Hongjiadu hydropower